

Automatic Control of Cycling Induced by Functional Electrical Stimulation With Electric Motor Assistance

Matthew J. Bellman, Ryan J. Downey, Anup Parikh, and Warren E. Dixon

Abstract—Cycling induced by automatic control of functional electrical stimulation provides a means of therapeutic exercise and functional restoration for people affected by paralysis. During cycling induced by functional electrical stimulation, various muscle groups are stimulated according to the cycle crank angle; however, because of kinematic constraints on the cycle-rider system, stimulation is typically only applied in a subsection of the crank cycle. Therefore, these systems can be considered as switched control systems with autonomous, state-dependent switching with potentially unstable modes. Previous studies have included an electric motor in the system to provide additional control authority, but no studies have considered the effects of switched control in the stability analysis of the motorized functional electrical stimulation cycling system. In this paper, a model of the motorized cycle-rider system with functional electrical stimulation is developed that includes the effects of a switched control input. A novel switching strategy for the electric motor is designed to only provide assistance in the regions of the crank cycle where the kinematic effectiveness of the rider's muscles is low. A switched sliding-mode controller is designed, and global, exponentially stable tracking of a desired crank trajectory is guaranteed via Lyapunov methods for switched systems, despite parametric uncertainty in the nonlinear model and unknown, time-varying disturbances. Experimental results from five able-bodied, passive riders are presented to validate the control design, and the developed control system achieves an average cadence tracking error of 0.00 ± 2.91 revolutions per minute for a desired trajectory of 50 revolutions per minute.

Note to Practitioners—Autonomous systems designed for rehabilitation and functional assistance for people with disabilities such as paralysis have the potential to maximize rehabilitative outcomes and improve the quality of life for millions of people. Disorders such as paralysis drastically reduce a person's ability to complete tasks due to a loss of neuromuscular control. Functional electrical stimulation can activate paralyzed muscles, restoring functional ability through automated application of electric current to the neuromuscular system, and, when applied to a task such as cycling, is both rehabilitative and empowering. However, cycling induced by functional electrical stimulation is limited by the capability of the rider's muscles, so an electric motor is typically added to accommodate the rider's ability and to support stability. The response by muscle to electrical stimulation is

uncertain, time-varying, and nonlinear, and switching the control input across multiple muscle groups and between the rider and an electric motor make guaranteeing stability and performance challenging. This paper presents a novel approach to the challenge of controlling motorized cycling systems with functional electrical stimulation that considers the switching effects and guarantees exponentially stable tracking of a desired crank trajectory, and experimental results indicate how the control system may be applied to a rehabilitative cycling task. Directions for future research are aimed at implementation of the developed control system in patient populations with paralysis to quantify its impact on therapeutic outcomes such as muscle function and neuroplasticity.

Index Terms—Functional electrical stimulation (FES), human-robot interaction, Lyapunov methods, medical control systems, rehabilitation robotics, switched control.

I. INTRODUCTION

REHABILITATIVE and assistive robotics focus on the design of autonomous systems to accommodate varying levels of functional ability for people with disabilities caused by injury or disease, either during a rehabilitative task or an activity of daily living [1], [2]. Rehabilitative robots typically enable people to perform a repetitive, therapeutic activity that they otherwise could not successfully perform (e.g., locomotor training for people with neurological disorders [3]), while assistive robots enable people to perform activities of daily living outside of a rehabilitative setting (e.g., walking outdoors). These systems must be designed to provide assistance in the regions of the task space where a person is functionally disabled, and should only provide input as needed to maximize efficiency and to ensure the person's participation in completing the task. Such human-centered autonomous systems have the potential to maximize therapeutic outcomes and enhance the quality of life for people with disabilities.

Paralysis is an example of a functional disability that rehabilitative and assistive robotic systems seek to mitigate. Autonomous systems that aid people with paralysis provide substitutionary motor control, typically via a system of artificial actuators (e.g., electric motors, hydraulic pistons) in the form of a robotic exoskeleton (e.g., [4] and [5]) or via functional electrical stimulation (FES), which activates paralyzed muscles by directing electric current into the neuromuscular complex and artificially inducing muscle contractions [6]. When FES is used to induce cycling as a functional activity, it is both rehabilitative and assistive [7]. When an able-bodied individual cycles voluntarily, the rider's leg muscles contract rhythmically to produce a pedaling motion. Meanwhile, paralyzed riders are unable to activate and coordinate their muscles to achieve cycling. FES-cycling systems have been designed to stimulate paralyzed

Manuscript received October 01, 2015; revised January 18, 2016; accepted January 23, 2016. Date of publication February 29, 2016; date of current version April 05, 2017. This paper was recommended for publication by Associate Editor T. Kawahara and Editor D. Tilbury upon evaluation of the reviewers' comments. This work was conducted with Government support under FA9550-11-C-0028 and awarded by the Department of Defense, Air Force Office of Scientific Research, National Defense Science and Engineering Graduate (NDSEG) Fellowship, 32 CFR 168a, and was supported in part by the National Science Foundation (NSF) Award under Grant 1161260.

The authors are with the Department of Mechanical and Aerospace Engineering, University of Florida, Gainesville FL 32611-6250 USA (e-mail: mattjo@ufl.edu; tenghu@ufl.edu; ryan2318@ufl.edu; wdixon@ufl.edu).

Color versions of one or more of the figures in this paper are available online at <http://ieeexplore.ieee.org>.

Digital Object Identifier 10.1109/TASE.2016.2527716

muscles according to a predefined stimulation pattern to enable cycling [8]–[13]. Stimulation patterns are designed in the joint space for cycling and include mappings from the crank position and velocity (cadence) to activation signals for each of the rider's muscle groups. Within the joint space are kinematic dead points, where only a small percentage of torque produced by the rider's muscles translates to torque about the crank axis. Stimulation patterns are typically designed such that FES is not applied in regions about these dead points. With such stimulation patterns, the nonlinear, uncertain FES-cycling system becomes a switched control system with autonomous, state-dependent switching and unstable modes [14], [15]. Indeed, the preliminary results in [16]–[18] demonstrate that potentially unstable modes do exist in FES-cycling systems when there are portions of the crank cycle where no stimulation is applied to the rider's muscle groups, as is common in existing FES-cycling systems.

FES-cycling systems that include electric motor assistance have been designed to facilitate controllability [10], [12], [19]–[25], as an electric motor has control authority across the entire joint space (i.e., not limited by dead points). In [19], an electric motor was added to ensure that the FES-cycling cadence did not fall below 25 revolutions per minute (rpm) and supplied a constant 5 Watts of power to compensate for losses in gearing. Similarly, in [20], a fuzzy logic control scheme was used to control a motor and FES to achieve a desired cadence. In [10], a motor controlled the cycling cadence while open-loop stimulation was applied to the rider's muscles to maximize power output. Similarly, in [12] and [21]–[25], electric motors were used to maintain a desired cadence, while FES was used to track a desired power output. None of the previous works considered the effects of the switching stimulation pattern on the motorized FES-cycling system's stability, so it is unclear how switching affects the system performance in general. Furthermore, all of these studies used the motor throughout the entire crank cycle, which may bias the control input towards the motor, potentially limiting the contribution from the rider's muscles and thereby limiting the therapeutic effects of the activity. Designing switched FES control systems with electric motor assistance that account for these factors may lead to more effective rehabilitative and assistive systems.

The previous work in [18] presented the development, stability analysis, and experimental validation of a controller for an FES-cycling system without an electric motor input. Ultimately bounded tracking of the desired cadence was guaranteed, and experimental results on able-bodied subjects demonstrated a cadence tracking error of 5.27 ± 2.14 rpm during FES-cycling at a desired cadence of 50 rpm. To improve tracking performance and eliminate unstable modes during FES-cycling, in this paper, a model of the motorized FES-cycling system is presented that includes the effects of switching the control input between an electric motor and FES of multiple muscle groups during cycling. Motivated by the desire to maximize the contribution of the rider's muscles, a novel strategy for electric motor assistance is developed that only provides control input in the regions around the dead points where no FES control input is provided. Based on this model, a switched, sliding-mode controller is developed for both the FES and the motor that yields global, exponentially stable tracking of a desired crank trajectory, despite the switching effects, uncertainty in the system parameters, and the

presence of unknown, bounded disturbances. Experimental results with five able-bodied subjects are presented to validate the controller and to demonstrate practical application of the theoretical insights, and the developed control system achieves an average cadence tracking error of 0.00 ± 2.91 rpm for a desired trajectory of 50 rpm, greatly improving the performance of the FES-cycling system as compared to the previous work in [18].

II. MODEL

A. Motorized Cycle-Rider System

The motorized cycle-rider system can be modeled as in [26] as

$$M\ddot{q} + V\dot{q} + G - \tau_p - \tau_b - \tau_d = \sum_{m \in \mathcal{M}} B_m u_m + B_e u_e \quad (1)$$

where $q \in \mathcal{Q} \subseteq \mathbb{R}$ denotes the crank angle; M , V , $G \in \mathbb{R}$ denote inertial, centripetal and Coriolis, and gravitational effects, respectively; τ_p , τ_b , $\tau_d \in \mathbb{R}$ denote the torques applied about the crank axis by passive viscoelastic tissue forces, viscous crank joint damping, and disturbances (e.g., spasticity or changes in load), respectively; $B_m \in \mathbb{R}$ denotes the control effectiveness for the electrically stimulated muscle group with subscript $m \in \mathcal{M} \triangleq \{RGlute, RQuad, RHam, LGlute, LQuad, LHam\}$ indicating the right (R) and left (L) gluteal ($Glute$), quadriceps femoris ($Quad$), and hamstrings (Ham) muscle groups; $u_m \in \mathbb{R}$ denotes the electrical stimulation intensity applied to each muscle group; $B_e \in \mathbb{R}$ is a constant relating the current in the electric motor's windings to the resulting torque about the crank axis; and $u_e \in \mathbb{R}$ is the control current applied to the electric motor windings.

Viscous damping in the cycle crank is modeled as $\tau_b \triangleq -c\dot{q}$, where $c \in \mathbb{R}_{>0}$ is an unknown viscous damping coefficient. The passive viscoelastic effects of the tissues surrounding the hip and knee joints can be expressed as

$$\tau_p \triangleq \sum_{j \in \mathcal{J}} T_j \tau_{j,p}$$

where $T_j \in \mathbb{R}$ are the joint torque transfer ratios [27] with subscript $j \in \mathcal{J} \triangleq \{RHip, RKnee, LHip, LKnee\}$ indicating right and left hip and knee joints, and $\tau_{j,p} \in \mathbb{R}$ denotes the resultant torque about the rider's joint from viscoelastic tissue forces. The joint torque transfer ratios can be expressed as

$$T_{*Hip} \triangleq -\frac{l_c}{l_t} \frac{\sin(q_{*Knee} - q)}{\sin(q_{*Knee} + q_{*Hip})}$$

$$T_{*Knee} \triangleq \frac{l_c}{l_l l_t} \left[\frac{l_t \sin(q_{*Knee} - q) - l_t \sin(q_{*Hip} + q)}{\sin(q_{*Knee} + q_{*Hip})} \right]$$

where l_t , l_l , $l_c \in \mathbb{R}_{>0}$ are the thigh and shank lengths of the rider and the cycle crank arm length, respectively, and the notation $*$ indicates that the expression holds for both right and left sides of the model (i.e., $*$ can be replaced by R or L to create distinct expressions). Based on [28] and [29], $\tau_{j,p}$ can be modeled as

$$\tau_{j,p} \triangleq k_{j,1} \exp(k_{j,2} \gamma_j) (\gamma_j - k_{j,3}) + b_{j,1} \tanh(-b_{j,2} \dot{\gamma}_j) - b_{j,3} \dot{\gamma}_j$$

for $j \in \mathcal{J}$, where $k_{j,i}$, $b_{j,i} \in \mathbb{R}$, $i \in \{1, 2, 3\}$, are unknown constant coefficients, and $\gamma_j \in \mathbb{R}$ denote the relative hip and knee joint angles, defined as

$$\gamma_{*Hip} \triangleq q_{*Hip} - q_t + \pi, \gamma_{*Knee} \triangleq q_{*Hip} - q_{*Knee}$$

where $q_t \in \mathbb{R}$ is the measurable, constant trunk angle.

The control effectiveness for each muscle group can be defined as

$$B_m \triangleq \Omega_m T_m$$

where $\Omega_m \in \mathbb{R}$ denotes the relationship between stimulation intensity and a muscle group's resultant torque about the joint it spans, and $T_m \in \mathbb{R}$ denotes the torque transfer ratio for a muscle group, which can be determined according to the primary joint that each muscle group spans as $T_{*Glute} = T_{*Hip}$, $T_{*Quad} = T_{*Ham} = T_{*Knee}$, given that the following assumption holds.

Assumption 1: The biarticular effects of the rectus femoris and hamstring muscles are negligible.

The uncertain function Ω_m is modeled as [30]

$$\Omega_m \triangleq \lambda_m \eta_m \cos(a_m)$$

for $m \in \mathcal{M}$, where $\lambda_m \in \mathbb{R}$ denotes the uncertain moment arm of a muscle's output force about the joint it spans, $\eta_m \in \mathbb{R}$ denotes the uncertain nonlinear function relating stimulation intensity to muscle fiber force, and $a_m \in \mathbb{R}$ denotes the uncertain pennation angle of the muscle fibers.

Property 1: The moment arm of the muscle group about the joint it spans λ_m , $\forall m \in \mathcal{M}$, depends on the joint angle and is nonzero and continuously differentiable with a bounded first time derivative [31].

Property 2: The function relating stimulation voltage to muscle fiber force η_m , $\forall m \in \mathcal{M}$, depends on the force-length and force-velocity relationships of the muscle being stimulated and is lower and upper bounded by known positive constants $c_{\eta 1}$, $c_{\eta 2} \in \mathbb{R}_{>0}$, respectively, provided the muscle is not fully stretched [32] or contracting concentrically at its maximum shortening velocity.

Property 3: The muscle fiber pennation angle $a_m \neq (n\pi + \pi/2)$, $\forall m \in \mathcal{M}$, $\forall n \in \mathbb{Z}$ (i.e., $\cos(a_m) \neq 0$) [33].

Property 4: Based on Properties 1–3, the function relating voltage applied to a muscle group and the resulting torque about the joint is nonzero and bounded. In other words, $0 < c_\omega < |\Omega_m| \leq c_\Omega$, $\forall m \in \mathcal{M}$, where c_ω , $c_\Omega \in \mathbb{R}_{>0}$ are known positive constants.

The control effectiveness for the electric motor is defined as $B_e \triangleq K_\tau r_g$, where $K_\tau \in \mathbb{R}_{>0}$ is the uncertain, constant coefficient relating armature current to torque, and $r_g \in \mathbb{R}_{>0}$ is the uncertain gear ratio between the motor output and the crank axis. It is assumed that $0 < c_e \leq B_e$, where $c_e \in \mathbb{R}_{>0}$ is a known constant.

B. Switched System Model

The control input can be generated by stimulation of the muscle groups or by an electric motor. A common question that arises in human-machine interaction is: How should the person's effort be balanced with the machine to accomplish

a task cooperatively? In this case, the person's effort is the electrically stimulated muscle input and the machine's is the electric motor input. For FES-cycling, stimulation is typically applied to each muscle group in a predefined region of the crank cycle where the muscles can contribute to the forward pedaling motion, and the muscles are not stimulated in regions of relatively low kinematic effectiveness (i.e., where the torque transfer ratios are small). On the other hand, an electric motor coupled to the crank shaft is able to provide consistent input throughout the entire crank cycle. In a rehabilitative setting, it is preferred that the muscles exert as much work to complete the cycling task as possible to maximize therapeutic effect; therefore, motivation arises to activate the electric motor only as needed. In the present development, the human-machine effort is balanced by only activating the muscle groups where they can effectively contribute to pedaling and activating the electric motor everywhere else. Switching the control input in this manner yields an autonomous, state-dependent, switched control system [14].

The portion of the crank cycle over which a particular muscle group is stimulated is denoted $\mathcal{Q}_m \subset \mathcal{Q}$ for $m \in \mathcal{M}$. Similarly, the portion of the crank cycle over which the electric motor actively contributes torque is denoted $\mathcal{Q}_e \subset \mathcal{Q}$. In this development, \mathcal{Q}_m is defined for each muscle group as

$$\mathcal{Q}_{*Glute} \triangleq \{q \in \mathcal{Q} \mid T_{*Glute}(q) > \varepsilon_{*Glute}\} \quad (2)$$

$$\mathcal{Q}_{*Quad} \triangleq \{q \in \mathcal{Q} \mid -T_{*Quad}(q) > \varepsilon_{*Quad}\} \quad (3)$$

$$\mathcal{Q}_{*Ham} \triangleq \{q \in \mathcal{Q} \mid T_{*Ham}(q) > \varepsilon_{*Ham}\} \quad (4)$$

where $\varepsilon_m \in (0, \max(T_m)]$ is a time-varying signal defined for $m \in \mathcal{M}$. Defining the stimulation regions as in (2)–(4) limits stimulation to portions of the crank cycle where the ratio of the torque produced by stimulation of the muscle group and the resultant torque about the crank axis is bounded below by ε_m , which is designed a priori, and prevents backpedaling, as the muscle groups may only be stimulated when the resultant torque about the crank axis is positive (i.e., forward pedaling). Note that a negative sign is included in (3) because knee extensor torque is defined to be negative. In this development, $\mathcal{Q}_e \triangleq \mathcal{Q} \setminus \mathcal{Q}_{FES}$, where $\mathcal{Q}_{FES} \triangleq \cup_{m \in \mathcal{M}} \mathcal{Q}_m$; in other words, the electric motor provides control input where the muscle groups do not. Based on these switching laws, a piecewise constant switching signal can be developed for each muscle group, $\sigma_m \in \{0, 1\}$, and for the electric motor, $\sigma_e \in \{0, 1\}$ as

$$\sigma_m \triangleq \begin{cases} 1, & \text{if } q \in \mathcal{Q}_m \\ 0, & \text{if } q \notin \mathcal{Q}_m \end{cases}, \quad \sigma_e \triangleq \begin{cases} 1, & \text{if } q \in \mathcal{Q}_e \\ 0, & \text{if } q \notin \mathcal{Q}_e \end{cases}. \quad (5)$$

Using these state-dependent switching signals, the stimulation input to the muscles groups and the current input to the motor windings can be defined as

$$u_m \triangleq k_m \sigma_m u, \quad u_e \triangleq k_e \sigma_e u \quad (6)$$

where k_m , $k_e \in \mathbb{R}_{>0}$, $m \in \mathcal{M}$, are positive, constant control gains, and $u \in \mathbb{R}$ is the subsequently designed control input. Substituting (6) into (1) and rearranging terms yields

$$M\ddot{q} + V\dot{q} + G - \tau_p - \tau_b - \tau_d = B_\sigma u \quad (7)$$

where $B_\sigma \in \mathbb{R}_{>0}$ is the lumped, switched control effectiveness term defined as

$$B_\sigma \triangleq \sum_{m \in \mathcal{M}} B_m k_m \sigma_m + B_e k_e \sigma_e.$$

Stimulation of six muscle groups allows for $2^6 = 64$ possible combinations of active muscle groups, including the empty set (i.e., the region where no stimulation is applied). The definitions in (2)–(6) introduce constraints that permit at most 28 different subsystems (i.e., B_σ may switch up to 28 times over a crank cycle), so that an auxiliary switching signal can be defined as $\sigma \in \mathcal{P} \triangleq \{1, 2, 3, \dots, 28\}$, where the first 27 subsystems represent some combination of active muscle groups and the 28th represents only electric motor activation. The switching signal σ specifies the index of B_σ and switches according to the crank position. For example, if only the right and left quadriceps femoris muscle groups were stimulated according to (3) and the electric motor was activated elsewhere, there would be only three subsystems, and σ would be defined as

$$\sigma \triangleq \begin{cases} 1, & \text{if } q \in \mathcal{Q}_{RQquad} \\ 2, & \text{if } q \in \mathcal{Q}_{LQquad} \\ 3, & \text{if } q \in \mathcal{Q}_e. \end{cases}$$

The known sequence of switching states, which are the limit points of $\mathcal{Q}_m, \forall m \in \mathcal{M}$, is defined as $\{q_n\}$, $n \in \{0, 1, 2, \dots\}$, and the corresponding sequence of unknown switching times $\{t_n\}$ is defined such that each t_n denotes the instant when q reaches the corresponding switching state q_n . The switching signal σ is assumed to be continuous from the right (i.e., $\sigma(q) = \lim_{q \rightarrow q_n^+} \sigma(q)$). The switched system in (7) has the following properties.

Property 5: $c_m \leq M \leq c_M$, where $c_m, c_M \in \mathbb{R}_{>0}$ are known constants.

Property 6: $|V| \leq c_V |\dot{q}|$, where $c_V \in \mathbb{R}_{>0}$ is a known constant.

Property 7: $|G| \leq c_G$, where $c_G \in \mathbb{R}_{>0}$ is a known constant.

Property 8: $|\tau_p| \leq c_{P1} + c_{P2} |\dot{q}|$, where $c_{P1}, c_{P2} \in \mathbb{R}_{>0}$ are known constants.

Property 9: $|\tau_b| \leq c_b |\dot{q}|$, where $c_b \in \mathbb{R}_{>0}$ is a known constant.

Property 10: $|\tau_d| \leq c_d$, where $c_d \in \mathbb{R}_{>0}$ is a known constant.

Property 11: $c_{B1} \leq B_\sigma \leq c_{B2}, \forall \sigma \in \mathcal{P}$, where $c_{B1}, c_{B2} \in \mathbb{R}_{>0}$ are known constants.

Property 12: $\dot{M} - 2V = 0$.

III. CONTROL DEVELOPMENT

The control objective is to track a desired crank trajectory with performance quantified by the tracking error signals $e_1, e_2 \in \mathbb{R}$, defined as

$$e_1 \triangleq q_d - q \quad (8)$$

$$e_2 \triangleq \dot{e}_1 + \alpha e_1 \quad (9)$$

where $q_d \in \mathbb{R}$ is the desired crank position, designed so that its derivatives exist and $\dot{q}_d, \ddot{q}_d \in \mathcal{L}_\infty$, and $\alpha \in \mathbb{R}_{>0}$ is a selectable constant. Without loss of generality, q_d is designed to monotonically

increase (i.e., backpedaling is not desired). Taking the time derivative of (9), multiplying by M , and using (7)–(9) yields

$$M\dot{e}_2 = \chi - e_1 - V e_2 - B_\sigma u \quad (10)$$

where the auxiliary term $\chi \in \mathbb{R}$ is defined as

$$\chi \triangleq M(\ddot{q}_d + \alpha \dot{e}_1) + V(\dot{q}_d + \alpha e_1) + G - \tau_p - \tau_b - \tau_d + e_1. \quad (11)$$

From Properties 5–10, χ can be bounded as

$$|\chi| \leq c_1 + c_2 \|z\| + c_3 \|z\|^2 \quad (12)$$

where $c_1, c_2, c_3 \in \mathbb{R}_{>0}$ are known constants, $\|\cdot\|$ denotes the Euclidean norm, and the error vector $z \in \mathbb{R}^2$ is defined as

$$z \triangleq [e_1 \quad e_2]^T.$$

Based on (10) and the subsequent stability analysis, the control input is designed as

$$u \triangleq k_1 e_2 + \left(k_2 + k_3 \|z\| + k_4 \|z\|^2\right) \text{sgn}(e_2) \quad (13)$$

where $\text{sgn}(\cdot)$ denotes the signum function and $k_1, k_2, k_3, k_4 \in \mathbb{R}_{>0}$ are constant control gains. Substituting (13) into (10) yields

$$M\dot{e}_2 = \chi - e_1 - V e_2 - B_\sigma \left[k_1 e_2 + \left(k_2 + k_3 \|z\| + k_4 \|z\|^2\right) \text{sgn}(e_2) \right]. \quad (14)$$

IV. STABILITY ANALYSIS

Let $V_L : \mathbb{R}^2 \rightarrow \mathbb{R}$ denote a continuously differentiable, positive definite, common Lyapunov function candidate defined as

$$V_L \triangleq \frac{1}{2} e_1^2 + \frac{1}{2} M e_2^2. \quad (15)$$

The common Lyapunov function candidate V_L satisfies the following inequalities:

$$\lambda_1 \|z\|^2 \leq V_L \leq \lambda_2 \|z\|^2 \quad (16)$$

where $\lambda_1, \lambda_2 \in \mathbb{R}_{>0}$ are known constants defined as

$$\lambda_1 \triangleq \min\left(\frac{1}{2}, \frac{c_m}{2}\right), \quad \lambda_2 \triangleq \max\left(\frac{1}{2}, \frac{c_M}{2}\right).$$

Theorem 1: The closed-loop error system in (14) is globally, exponentially stable in the sense that

$$\|z\| \leq \sqrt{\frac{\lambda_2}{\lambda_1}} \|z(t_0)\| \exp\left[-\frac{1}{2} \lambda_s (t - t_0)\right] \quad (17)$$

for all $t \in [t_0, \infty)$, where $t_0 \in \mathbb{R}_{\geq 0}$ is the initial time, and $\lambda_s \in \mathbb{R}_{>0}$ is defined as

$$\lambda_s \triangleq \frac{1}{\lambda_2} \min(\alpha, c_{B1} k_1) \quad (18)$$

provided the following gain conditions are satisfied:

$$k_2 \geq \frac{c_1}{c_{B1}}, \quad k_3 \geq \frac{c_2}{c_{B1}}, \quad k_4 \geq \frac{c_3}{c_{B1}}. \quad (19)$$

Proof: Consider $\sigma = p$ for some arbitrary $p \in \mathcal{P}$ such that B_p is continuous. Because of the signum function in u , the

time derivative of (15) exists almost everywhere (a.e.), i.e., for almost all $t \in [t_n, t_{n+1})$, $n \in \{0, 1, 2, \dots\}$. Therefore, after substituting (14), utilizing Property 12, and rearranging terms, the time derivative of (15) can be expressed as

$$\dot{V}_L \stackrel{a.e.}{=} \dot{e}_1 e_1 - e_1 e_2 + \chi e_2 - B_p k_1 e_2 - B_p \left(k_2 + k_3 \|z\| + k_4 \|z\|^2 \right) \text{sgn}(e_2) e_2.$$

Using (9), (12), and Property 11, it can be demonstrated that

$$\dot{V}_L \stackrel{a.e.}{\leq} -\alpha e_1^2 - c_{B1} k_1 e_2^2 - (c_{B1} k_2 - c_1) |e_2| - (c_{B1} k_3 - c_2) \|z\| |e_2| - (c_{B1} k_4 - c_3) \|z\|^2 |e_2|. \quad (20)$$

Provided the gain conditions in (19) are satisfied, (16) can be used to rewrite (20) as

$$\dot{V}_L \stackrel{a.e.}{\leq} -\lambda_s V_L, \quad (21)$$

where λ_s was defined in (18). The inequality in (21) can be rewritten as

$$\exp[\lambda_s (t - t_n)] \left(\dot{V}_L + \lambda_s V_L \right) \stackrel{a.e.}{\leq} 0$$

for $t \in [t_n, t_{n+1})$, which is equivalent to the following expression:

$$\frac{d}{dt} \{ V_L \exp[\lambda_s (t - t_n)] \} \stackrel{a.e.}{\leq} 0. \quad (22)$$

Taking the Lebesgue integral of (22) and recognizing that the integrand on the left-hand side is absolutely continuous allows the Fundamental Theorem of Calculus to be used to yield

$$V_L \leq V_L(t_n) \exp[-\lambda_s (t - t_n)] \quad (23)$$

for $t \in [t_n, t_{n+1})$.

Since (23) was proven to hold for an arbitrary σ , (23) holds for all $\sigma \in \mathcal{P}$. Therefore, V_L is indeed a common Lyapunov function, and (23) holds for all $t \in [t_0, \infty)$. In other words

$$V_L \leq V_L(t_0) \exp[-\lambda_s (t - t_0)]. \quad (24)$$

Using (16) to bound (24) and performing some algebraic manipulation yields (17). ■

Remark 1: The exponential decay rate λ_s represents the most conservative (i.e., smallest) decay rate for the closed-loop, switched error system. In practice, each subsystem has its own decay rate dependent on the lower bound of the corresponding B_σ , but in the preceding stability analysis, c_{B1} was used as the lower bound on B_σ for all $\sigma \in \mathcal{P}$. Fig. 1 illustrates how V_L may behave in practice versus the conservative bound given in (24).

V. EXPERIMENTS

Experiments were conducted with the primary objective of evaluating the performance of the controller given in (13) and distributed as FES and electric motor current according to (3)–(6). Five able-bodied subjects (four male, one female) 21–43 years old participated in the experiments. Each subject gave written informed consent approved by the University of Florida Institutional Review Board. During the subsequent experiments, the subjects were instructed to relax and make no

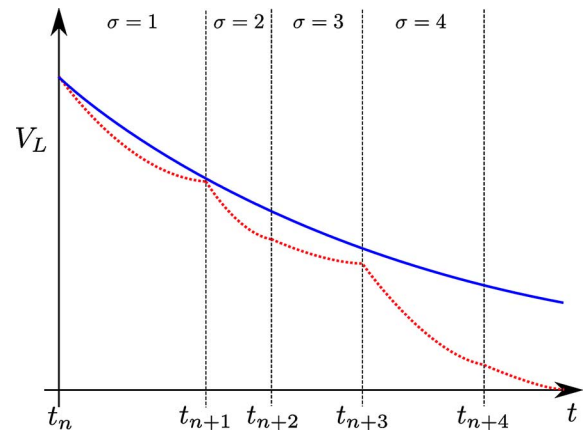


Fig. 1. Illustration of the behavior of V_L . The solid line represents the bound given in (24), and the dotted line represents an example of how V_L may behave in practice.



Fig. 2. Motorized FES-cycling test bed. (A) Electric motor. (B) Stimulator. (C) Orthotic pedals.

volitional effort to either assist or inhibit the FES or the electric motor input (i.e., passive riders).

A. Motorized FES-Cycling Test Bed

A commercially available recumbent tricycle (TerraTrike Rover) was modified for the purposes of the FES-cycling experiments. A 250 Watt, brushed, 24 VDC electric motor (Unite Motor Co. Ltd. MY1016Z2) was mounted to the frame and coupled to the drive chain. Orthotic boots (Össur Rebound Air Tall) were affixed to custom pedals; these orthotic pedals served to fix the rider's feet to the pedals, prevent dorsiflexion and plantarflexion of the ankles, and maintain sagittal alignment of the lower legs. An optical encoder with an angular resolution of 0.018° (U.S. Digital H1) was coupled to the cycle crank via spur gears to measure the crank position. To make the system stationary, a stationary cycling trainer and riser rings (Kinetic by Kurt) were used to lift the tricycle's drive wheel off the ground. Current control of the cycle's motor was enabled by a general purpose linear amplifier (AE Techron LVC 5050) interfacing with the data acquisition hardware (Quanser Q8-USB), which also measured the encoder signal. The controller was implemented on a personal computer running real-time control software (QUARC, MATLAB/Simulink, Windows 7) at a sampling rate of 500 Hz. Fig. 2 depicts the motorized FES-cycling test bed.

A current-controlled stimulator (Hasomed RehaStim) delivered biphasic, symmetric, rectangular pulses to the subject's

muscle groups via bipolar, self-adhesive, PALS® electrodes.¹ The stimulation amplitudes were fixed at 90 mA for the quadriceps and 80 mA for the hamstrings muscle groups, and the stimulation pulse width for each muscle group was determined by u_m and commanded to the stimulator by the control software. Stimulation frequency was fixed at 60 Hz to leverage the results found in [34]. For safety, an emergency stop switch was attached to the tricycle that enabled the subject to stop the experiment immediately if necessary, though no subjects found it necessary.

B. Experimental Setup

Electrodes were placed over the subjects' quadriceps femoris and hamstrings muscle groups according to Axelgaard's electrode placement manual.² In these experiments, only the quadriceps and hamstrings muscle groups were stimulated to better demonstrate the balance between the FES and motor inputs. Each subject's legs were measured to obtain the distance from the greater trochanter to the lateral femoral condyle and from the lateral femoral condyle to the sole of the foot, while the ankle was held in the anatomically neutral position. Subjects were then seated on the tricycle, and their feet were inserted securely into the orthotic pedals. The tricycle's seat position was adjusted for each subject's comfort while ensuring that full extension of the knees could not be achieved while cycling, and the distance from the cycle crank to the subject's right greater trochanter was measured. These measurements were used to calculate the torque transfer ratios for the subjects' muscle groups and to thereby determine the stimulation pattern.

Two experimental protocols were conducted with each subject, and each trial lasted 180 s. In Protocol 1, the desired cadence rose to 50 rpm and remained there for the duration of the experiment, while in Protocol 2 the desired cadence first rose to 50 rpm, then varied sinusoidally from 40 to 60 rpm to demonstrate the robustness of the developed control system. For Protocol 1 the desired crank velocity \dot{q}_d and position q_d were designed as

$$\dot{q}_d \triangleq \frac{5\pi}{3} \left\{ 1 - \exp \left[-\frac{2}{5}(t - t_0) \right] \right\} \quad (25)$$

$$q_d \triangleq \frac{5\pi}{3} (t - t_0) - \frac{5}{2} \dot{q}_d + q(t_0) \quad (26)$$

where $t_0 = 0$ s. The trajectories in (25) and (26) ensured that the desired cadence started at 0 rpm and smoothly approached 50 rpm. For Protocol 2, the desired crank velocity \dot{q}_d and position q_d were designed as

$$\dot{q}_d \triangleq \begin{cases} \frac{5\pi}{3} \left[1 - \left(\frac{t-t_1}{t_1} \right)^4 \right] & t < t_1 \\ \frac{5\pi}{3} & t_1 \leq t < t_2 \\ \frac{\pi}{6} \cos \left[\frac{\pi}{15} (t - t_2) \right] + \frac{3\pi}{2} & t_2 \leq t < t_3 \\ -\frac{\pi}{3} \cos \left[\frac{\pi}{15} (t - t_3) \right] + \frac{5\pi}{3} & t \geq t_3 \end{cases} \quad (27)$$

¹Surface electrodes for this study were provided compliments of Axelgaard Manufacturing Co., Ltd.

²<http://www.palsclinicalsupport.com/videoElements/videoPage.php>

$$q_d \triangleq \begin{cases} \frac{5\pi}{3} \left[t - \frac{(t-t_1)^5 + t_1^5}{5t_1^4} \right] + q(t_0) & t < t_1 \\ \frac{5\pi}{3} (t - t_1) + q_d(t_1) & t_1 \leq t < t_2 \\ \frac{5}{2} \sin \left[\frac{\pi}{15} (t - t_2) \right] + \frac{3\pi}{2} (t - t_2) + q_d(t_2) & t_2 \leq t < t_3 \\ -5 \sin \left[\frac{\pi}{15} (t - t_3) \right] + \frac{5\pi}{3} (t - t_3) + q_d(t_3) & t \geq t_3, \end{cases} \quad (28)$$

where $t_1 \triangleq 16$ s, $t_2 \triangleq 26$ s, and $t_3 \triangleq 41$ s. The trajectories in (27) and (28) ensured that the desired cadence started at 0 rpm, smoothly approached 50 rpm, then varied sinusoidally from 40 to 60 rpm with a period of 30 s.

For both protocols, the signals ε_m were designed for $m \in \mathcal{M}$ as

$$\varepsilon_m \triangleq \max(I_m) \gamma \quad (29)$$

where $\gamma \in \mathbb{R}$ was a scaling factor designed as

$$\gamma \triangleq \begin{cases} 1, & t < t_1 \\ 1.4 - \frac{t}{40}, & t_1 \leq t < t_2 \\ 0.75, & t \geq t_2. \end{cases} \quad (30)$$

By defining ε_m as in (29), the stimulation pattern was consistent across all subjects, despite differences in cycle-rider geometry. For example, Subject 1 had $l_t = 18$ inches and $l_l = 22.5$ inches and sat 31.4 inches away from the crank, whereas Subject 2 had $l_t = 15.5$ inches and $l_l = 22$ inches and sat 28.8 inches away from the crank. Despite the difference in cycle-rider geometry between subjects, Subject 1 had $\mathcal{Q}_{RQuad} = (68, 161)$ degrees,³ and Subject 2 had $\mathcal{Q}_{RQuad} = (69, 163)$ degrees. In addition to maintaining consistency in the stimulation pattern across subjects, the definitions in (29) and (30) determined the stimulation pattern and FES-to-motor switching according to (3)–(6), so that only the motor was active during the first 16 s of each trial (i.e., while the desired trajectory rose to 50 rpm). Then, the stimulation of the muscle groups was added and the stimulation regions increased in size for 10 s until they reached the desired steady state stimulation pattern.⁴ This method for defining the stimulation pattern was selected because large muscle forces are required to pedal at low speeds [35], so the motor was used to bring the system to the desired cadence before FES was added. A constant input of 0.5 A was added to the motor current input to mitigate the effect of friction in the motor gearbox. The control gains, introduced in (6) and (13), and the constant α , introduced in (9), were tuned to yield acceptable tracking performance prior to each trial and ranged as follows: $\alpha \in [7, 10]$, $k_m = 0.25 \forall m \in \mathcal{M}$, $k_e \in [5.75 \times 10^{-3}, 13.2]$, $k_1 \in [80, 100]$, $k_2 \in [4, 100]$, $k_3 = 0.01$, $k_4 = 0.001$.

C. Results

Fig. 3 depicts one subject's tracking performance during both protocols, quantified by e_1 , \dot{e}_1 , the stimulation intensity input to each muscle group u_m , and the electric motor current

³A crank angle of zero° was defined as the position where the right crank was horizontal and pointing towards the rider.

⁴Values of 16 and 26 s were selected to ensure that only the motor was active while the trajectory rose to 50 rpm and to allow for a smooth transition from passive (i.e., motor-only) cycling to FES-cycling.

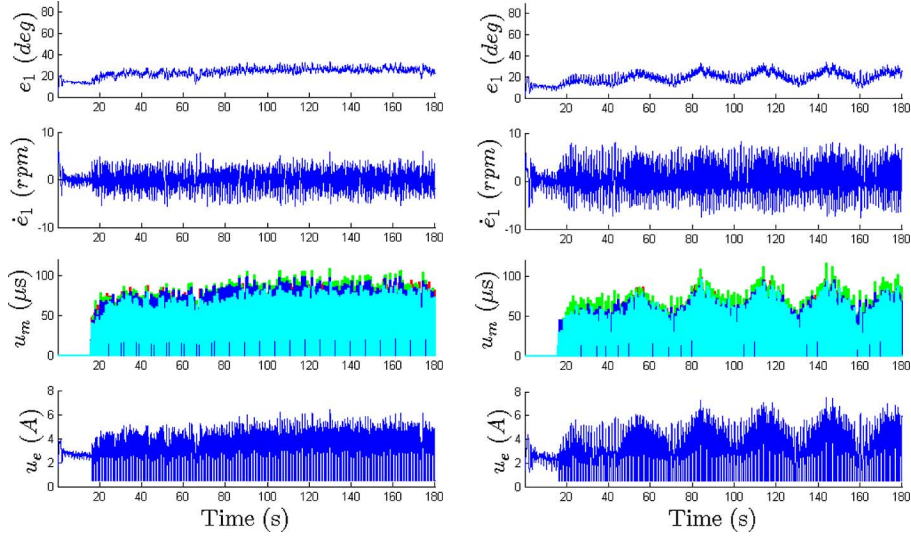


Fig. 3. Tracking performance for Subject 1 during Protocol 1 (left) and Protocol 2 (right), quantified by the position tracking error e_1 , cadence tracking error \dot{e}_1 , FES control input to each muscle group u_m , and electric motor current input u_e . Fig. 4 provides an enhanced view of the FES and electric motor control inputs.

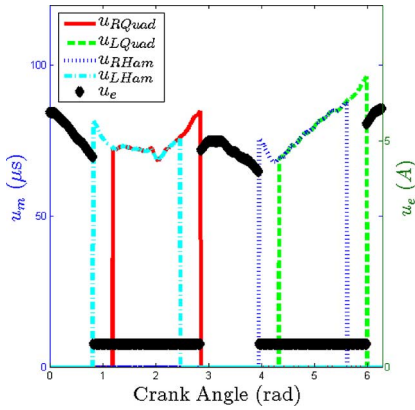


Fig. 4. FES control inputs u_m and motor current input u_e from one motorized FES-cycling trial over a single crank cycle.

input u_e . Fig. 4 provides an enhanced view of the distribution of the control input between FES and the motor across one crank cycle. Table I summarizes the position and cadence tracking performance for each subject during the motor-only ($t \in [t_0, t_1]$ seconds), transitory ($t \in [t_1, t_2]$ seconds), and FES/motor ($t \in [t_2, 180]$ seconds) periods of Protocol 1. Similarly, Table II summarizes the tracking performance for each subject during Protocol 2.

D. Discussion

The experimental results successfully demonstrate the ability of the controller in (13), distributed between FES of the rider's muscle groups and electric motor current according to (6), to achieve exponentially stable tracking performance despite parametric uncertainty (e.g., uncertain rider limb mass) and unknown disturbances. However, the results indicate exponential convergence to an ultimate bound on the tracking error, instead of convergence to zero, which could be due to unmodeled effects such as electromechanical delay between muscle activation and force production [36]. The results for Subject 1, presented in Fig. 3, demonstrate typical performance

TABLE I
SUMMARY OF MOTORIZED FES-CYCLING PERFORMANCE FOR ALL FIVE SUBJECTS DURING PROTOCOL 1. THE MEAN AND STANDARD DEVIATION (ST. DEV.) ARE PROVIDED FOR EACH SUBJECT'S POSITION TRACKING ERROR e_1 IN DEGREES AND CADENCE TRACKING ERROR \dot{e}_1 IN RPM FOR THE MOTOR-ONLY ($t \in [t_0, t_1]$ seconds), TRANSITORY ($t \in [t_1, t_2]$ seconds), AND FES/MOTOR ($t \in [t_2, 180]$ seconds) PERIODS OF THE TRIALS

		Motor-only		Transitory		FES/Motor	
		Mean	St. Dev.	Mean	St. Dev.	Mean	St. Dev.
Subject 1	e_1 (deg.)	13.70	2.36	18.72	2.86	24.38	2.90
	\dot{e}_1 (rpm)	0.34	1.32	0.11	2.12	-0.00	2.07
Subject 2	e_1 (deg.)	12.04	2.19	18.64	3.91	26.13	3.69
	\dot{e}_1 (rpm)	0.33	1.34	0.20	1.97	-0.00	2.68
Subject 3	e_1 (deg.)	10.61	2.73	15.13	3.29	17.48	2.80
	\dot{e}_1 (rpm)	0.31	1.73	0.13	2.77	0.00	3.44
Subject 4	e_1 (deg.)	13.83	2.57	21.85	3.77	33.25	4.59
	\dot{e}_1 (rpm)	0.36	1.75	0.24	2.56	0.01	2.82
Subject 5	e_1 (deg.)	5.98	2.55	10.74	3.36	15.18	2.69
	\dot{e}_1 (rpm)	0.25	2.11	0.13	3.09	0.01	3.52

during the motorized FES-cycling task, as corroborated by the data in Tables I and II. Of particular note is the mean and standard deviation of the cadence tracking error during the FES/motor period for all subjects, where the average cadence tracking error across all five subjects was 0.00 ± 2.91 rpm (i.e., the actual cadence was centered about the desired cadence with less than 3 rpm in standard deviation) for Protocol 1 and 0.01 ± 3.15 rpm for Protocol 2. In comparison, the average position tracking error across all five subjects was $23.28 \pm 3.33^\circ$ for Protocol 1 and $18.05 \pm 4.98^\circ$ for Protocol 2, indicating that the actual crank trajectory lagged the desired trajectory consistently across all experiments. The steady state offset in the position tracking error was likely caused by a bias in the tuning of the control gains towards improving cadence tracking performance, as cadence error is generally considered to be the main performance criterion during cycling tasks.

As indicated in the experimental data plotted in Fig. 4, the electric motor provided assistance as needed in the regions of the FES-cycling joint space where the rider's torque transfer

TABLE II

SUMMARY OF MOTORIZED FES-CYCLING PERFORMANCE FOR ALL FIVE SUBJECTS DURING PROTOCOL 2. THE MEAN AND STANDARD DEVIATION (ST. DEV.) ARE PROVIDED FOR EACH SUBJECT'S POSITION TRACKING ERROR e_1 IN DEGREES AND CADENCE TRACKING ERROR \dot{e}_1 IN RPM FOR THE MOTOR-ONLY ($t \in [t_0, t_1]$ seconds), TRANSITORY ($t \in [t_1, t_2]$ seconds), AND FES/MOTOR ($t \in [t_2, 180]$ seconds) PERIODS OF THE TRIALS

		Motor-only		Transitory		FES/Motor	
		Mean	St. Dev.	Mean	St. Dev.	Mean	St. Dev.
Subject 1	e_1 (deg.)	11.00	2.84	14.99	2.92	20.55	4.62
	\dot{e}_1 (rpm)	0.33	1.75	0.06	2.71	0.01	2.98
Subject 2	e_1 (deg.)	6.70	1.81	10.28	2.44	13.96	5.23
	\dot{e}_1 (rpm)	0.28	1.35	0.12	2.38	0.01	3.11
Subject 3	e_1 (deg.)	9.32	2.23	13.24	2.74	18.95	5.59
	\dot{e}_1 (rpm)	0.30	1.53	0.15	2.04	0.00	2.79
Subject 4	e_1 (deg.)	8.99	3.19	13.96	2.53	22.04	5.15
	\dot{e}_1 (rpm)	0.31	2.08	0.13	2.52	0.01	3.28
Subject 5	e_1 (deg.)	5.61	2.51	10.26	3.06	14.72	4.29
	\dot{e}_1 (rpm)	0.25	1.85	0.14	2.97	0.00	3.62

ratios were small, and stability was maintained throughout the trial despite the discontinuous switching in the torque input to the system. The subjects reported that the cycling motion felt comfortable and natural and that they perceived their muscles as contributing significantly to the cycling task, though neither metabolic nor relative torque contribution (i.e., comparing FES torque input to motor torque input) measurements were available to quantify these effects.

VI. CONCLUSION

A model for FES-cycling with electric motor assistance was presented that includes the effects of a switched control input and unknown disturbances. Based on this model, a novel switching strategy was developed that applies FES to the rider's muscle groups in regions of the crank cycle where the rider's muscles contribute significantly to the cycling task and utilizes an electric motor for assistance only as needed (i.e., in regions of poor kinematic efficiency). A switched sliding-mode controller was designed to yield global, exponentially stable tracking of a desired crank trajectory, provided sufficient gain conditions are satisfied. The control design was validated in experiments with five able-bodied subjects, where an average cadence tracking error of 0.00 ± 2.91 rpm ($0.00 \pm 5.82\%$ error) was demonstrated when tracking a constant desired cadence of 50 rpm.

The developed control system for motorized FES-cycling systems has the potential to enhance therapeutic outcomes in a rehabilitative setting and to improve the performance of assistive cycling devices; however, clinical implementation of the developed control system may present additional challenges not considered in this paper. FES-cycling is typically prescribed for the rehabilitation of people with spinal cord injury, stroke, or cerebral palsy. While the theoretical development in this paper considers a generalized cycle-rider system, applying the developed control system to a particular patient population may require disorder-specific tuning of the system parameters or the addition of disorder-specific functionality. A patient may be sensitive to FES and would therefore require lower limits on the stimulation intensity, potentially leading to control input saturation and requiring an extension of the developed

control system to consider saturation, as in [37]. If a patient has significant asymmetry in the lower limbs (e.g., hemiparetic stroke), a rehabilitative goal may be to improve symmetry during cycling, which may be accomplished by only applying FES to the affected limb and designing the desired trajectory to mimic the trajectory of the other limb, similar to the methods described in [38]. Future work will focus on applying the developed control system to people with neurological disorders and will necessarily consider such disorder-specific challenges to implementation. Further work also needs to involve clinical trials in clinically relevant patient populations to investigate training benefits.

ACKNOWLEDGMENT

Any opinions, findings and conclusions or recommendations expressed in this material are those of the authors and do not necessarily reflect the views of the sponsoring agency.

REFERENCES

- [1] N. Tejima, "Rehabilitation robotics: A review," *Adv. Robot.*, vol. 14, no. 7, pp. 551–564, 2000.
- [2] L. Marchal-Crespo and D. J. Reinkensmeyer, "Review of control strategies for robotic movement training after neurologic injury," *J. Neuroeng. Rehabil.*, vol. 6, no. 1, pp. 1–15, 2009.
- [3] C. Tefertiller, B. Pharo, N. Evans, and P. Winchester, "Efficacy of rehabilitation robotics for walking training in neurological disorders: A review," *J. Rehabil. Res. Dev.*, vol. 48, no. 4, pp. 387–416, 2011.
- [4] S. Jezernik, G. Colombo, and M. Morari, "Automatic gait-pattern adaptation algorithms for rehabilitation with a 4-dof robotic orthosis," *IEEE Trans. Robot. Autom.*, vol. 20, no. 3, pp. 574–582, Jun. 2004.
- [5] H. S. Lo and S. Q. Xie, "Exoskeleton robots for upper-limb rehabilitation: State of the art and future prospects," *Med. Eng. Phys.*, vol. 34, no. 3, pp. 261–268, Apr. 2012.
- [6] O. Schuhfried, R. Crevenna, V. Fialka-Moser, and T. Pater-nostro-Sluga, "Non-invasive neuromuscular electrical stimulation in patients with central nervous system lesions: An educational review," *J. Rehabil. Med.*, vol. 44, no. 2, pp. 99–105, Feb. 2012.
- [7] C.-W. Peng, S.-C. Chen, C.-H. Lai, C.-J. Chen, C.-C. Chen, J. Mizrahi, and Y. Handa, "Review: Clinical benefits of functional electrical stimulation cycling exercise for subjects with central neurological impairments," *J. Med. Biol. Eng.*, vol. 31, pp. 1–11, 2011.
- [8] J. S. Petrofsky, H. Heaton, and C. A. Phillips, "Outdoor bicycle for exercise in paraplegics and quadriplegics," *J. Biomed. Eng.*, vol. 5, pp. 292–296, Oct. 1983.
- [9] C. A. Phillips, J. S. Petrofsky, D. M. Hendershot, and D. Stafford, "Functional electrical exercise: A comprehensive approach for physical conditioning of the spinal cord injured patient," *Orthopedics*, vol. 7, no. 7, pp. 1112–1123, 1984.
- [10] M. Gföhler, T. Angeli, T. Eberharter, P. Lugner, W. Mayr, and C. Hofer, "Test bed with force-measuring crank for static and dynamic investigation on cycling by means of functional electrical stimulation," *IEEE Trans. Neural Syst. Rehabil. Eng.*, vol. 9, no. 2, pp. 169–180, Jun. 2001.
- [11] T. A. Perkins, N. N. Donaldson, N. A. C. Hatcher, I. D. Swain, and D. E. Wood, "Control of leg-powered paraplegic cycling using stimulation of the lumbro-sacral anterior spinal nerve roots," *IEEE Trans. Neural Syst. Rehabil. Eng.*, vol. 10, no. 3, pp. 158–164, Sep. 2002.
- [12] K. J. Hunt, B. Stone, N.-O. Negård, T. Schauer, M. H. Fraser, A. J. Cathcart, C. Ferrario, S. A. Ward, and S. Grant, "Control strategies for integration of electric motor assist and functional electrical stimulation in paraplegic cycling: Utility for exercise testing and mobile cycling," *IEEE Trans. Neural Syst. Rehabil. Eng.*, vol. 12, no. 1, pp. 89–101, Mar. 2004.
- [13] K. J. Hunt, C. Ferrario, S. Grant, B. Stone, A. N. McLean, M. H. Fraser, and D. B. Allan, "Comparison of stimulation patterns for FES-cycling using measures of oxygen cost and stimulation cost," *Med. Eng. Phys.*, vol. 28, no. 7, pp. 710–718, Sep. 2006.
- [14] D. Liberzon, *Switching in Systems and Control*. Boston, MA, USA: Birkhauser, 2003.

- [15] H. Yang, B. Jiang, and V. Cocquempot, "A survey of results and perspectives on stabilization of switched nonlinear systems with unstable modes," *Nonlin. Anal.: Hybrid Syst.*, vol. 13, pp. 45–60, Aug. 2014.
- [16] M. J. Bellman, T.-H. Cheng, R. J. Downey, and W. E. Dixon, "Stationary cycling induced by switched functional electrical stimulation control," in *Proc. Amer. Control Conf.*, 2014, pp. 4802–4809.
- [17] M. J. Bellman, T.-H. Cheng, R. Downey, and W. E. Dixon, "Cadence control of stationary cycling induced by switched functional electrical stimulation control," in *Proc. IEEE Conf. Decis. Control*, Los Angeles, CA, USA, 2014, pp. 6260–6265.
- [18] M. J. Bellman, T. H. Cheng, R. J. Downey, C. J. Hass, and W. E. Dixon, "Switched control of cadence during stationary cycling induced by functional electrical stimulation," *IEEE Trans. Neural Syst. Rehabil. Eng.*, to be published.
- [19] D. J. Pons, C. L. Vaughan, and G. G. Jaros, "Cycling device powered by the electrically stimulated muscles of paraplegics," *Med. Biol. Eng. Comput.*, vol. 27, no. 1, pp. 1–7, 1989.
- [20] Y. Ogawa, T. Inoue, T. Inada, Y. Tagawa, K. Yoshimitsu, and N. Shiba, "Locomotion assistance for the person with mobility impairment: Fuzzy control of cycling movement by means of surface electrical-stimulation," in *Proc. 29th Int. Conf. IEEE EMBS*, Aug. 2007, pp. 2420–2423.
- [21] C. Fornusek, G. M. Davis, P. J. Sinclair, and B. Milthorpe, "Development of an isokinetic functional electrical stimulation cycle ergometer," *Nueromodulation*, vol. 7, no. 1, pp. 56–64, 2004.
- [22] C. G. A. McRae, T. E. Johnston, R. T. Lauer, A. M. Tokay, S. C. K. Lee, and K. J. Hunt, "Cycling for children with neuromuscular impairments using electrical stimulation-development of tricycle-based systems," *Med. Eng. Phys.*, vol. 31, no. 6, pp. 650–659, 2009.
- [23] E. Ambrosini, S. Ferrante, T. Schauer, G. Ferrigno, F. Molteni, and A. Pedrocchi, "Design of a symmetry controller for cycling induced by electrical stimulation: Preliminary results on post-acute stroke patients," *Artif. Organs*, vol. 34, no. 8, pp. 663–667, Aug. 2010.
- [24] L. D. Duffell, N. d. N. Donaldson, and D. J. Newham, "Power output during functional electrically stimulated cycling in trained spinal cord injured people," *Neuromodulation: Technol. Neural Interface*, vol. 13, no. 1, pp. 50–57, 2010.
- [25] A. Farhoud and A. Erfanian, "Fully automatic control of paraplegic FES pedaling using higher-order sliding mode and fuzzy logic control," *IEEE Trans. Neural Syst. Rehabil. Eng.*, vol. 22, no. 3, pp. 533–542, May 2014.
- [26] E. S. Idsø, "Development of a mathematical model of a rider-tricycle system," Dept. Eng. Cybern., Norwegian Univ. Sci. Technol. (NTNU), Tech. Rep., 2002.
- [27] E. S. Idsø, T. Johansen, and K. J. Hunt, "Finding the metabolically optimal stimulation pattern for FES-cycling," in *Proc. Conf. Int. Funct. Electrical Stimulation Soc.*, Bournemouth, U.K., Sep. 2004.
- [28] M. Ferrarin and A. Pedotti, "The relationship between electrical stimulus and joint torque: A dynamic model," *IEEE Trans. Rehabil. Eng.*, vol. 8, no. 3, pp. 342–352, Sep. 2000.
- [29] T. Schauer, N. O. Negård, F. Previdi, K. J. Hunt, M. H. Fraser, E. Ferchland, and J. Raisch, "Online identification and nonlinear control of the electrically stimulated quadriceps muscle," *Control Eng. Pract.*, vol. 13, no. 9, pp. 1207–1219, Sep. 2005.
- [30] N. Sharma, K. Stegath, C. M. Gregory, and W. E. Dixon, "Nonlinear neuromuscular electrical stimulation tracking control of a human limb," *IEEE Trans. Neural Syst. Rehabil. Eng.*, vol. 17, no. 6, pp. 576–584, Jun. 2009.
- [31] J. L. Krevolin, M. G. Pandy, and J. C. Pearce, "Moment arm of the patellar tendon in the human knee," *J. Biomech.*, vol. 37, no. 5, pp. 785–788, 2004.
- [32] D. A. Winter, *Biomechanics and Motor Control of Human Movement*. New York, NY, USA: Wiley, 1990.
- [33] O. M. Rutherford and D. A. Jones, "Measurement of fibre pennation using ultrasound in the human quadriceps in vivo," *Eur. J. Appl. Physiol. Occup. Physiol.*, vol. 65, pp. 433–437, 1992.
- [34] P. C. Eser, N. Donaldson, H. Knecht, and E. Stussi, "Influence of different stimulation frequencies on power output and fatigue during FES-cycling in recently injured SCI people," *IEEE Trans. Neural Syst. Rehabil. Eng.*, vol. 11, no. 3, pp. 236–240, Sep. 2003.
- [35] C. Fornusek and G. M. Davis, "Maximizing muscle force via low-cadence functional electrical stimulation cycling," *J. Rehabil. Med.*, vol. 36, pp. 232–237, 2004.
- [36] N. Sharma, C. Gregory, and W. E. Dixon, "Predictor-based compensation for electromechanical delay during neuromuscular electrical stimulation," *IEEE Trans. Neural Syst. Rehabil. Eng.*, vol. 19, no. 6, pp. 601–611, Dec. 2011.
- [37] N. Fischer, Z. Kan, R. Kamalapurkar, and W. E. Dixon, "Saturated RISE feedback control for a class of second-order nonlinear systems," *IEEE Trans. Autom. Control*, vol. 59, no. 4, pp. 1094–1099, Apr. 2014.
- [38] E. Ambrosini, S. Ferrante, G. Ferrigno, F. Molteni, and A. Pedrocchi, "Cycling induced by electrical stimulation improves muscle activation and symmetry during pedaling in hemiparetic patients," *IEEE Trans. Neural Syst. Rehabil. Eng.*, vol. 20, no. 3, pp. 320–330, May 2012.



Matthew J. Bellman received the bachelor's and master's degrees (*magna cum laude*) in mechanical engineering with a minor in biomechanics and the Ph.D. degree in mechanical engineering as a National Defense Science and Engineering (NDSEG) Fellow from the University of Florida, Gainesville, FL, USA.

He is a member of the Nonlinear Controls and Robotics Group since May 2009. His focus is on the theoretical development of robust, adaptive control systems for applications involving functional

electrical stimulation, specifically those involving rehabilitation and mobility of the lower extremities.

Dr. Bellman was the recipient of the 2015 American Automatic Control Council (AACC) O. Hugo Schuck (Best Paper) Award.



Ryan J. Downey received the B.S. degree in mechanical engineering from the University of Florida, Gainesville, FL, USA, in 2010, where he participated in a research experiences for undergraduates program (REU). He subsequently joined the Nonlinear Controls and Robotics Group in 2010 to pursue his doctoral research. In 2011, he was accepted to an international exchange program (Atlantis CRISP) and received the M.S. degree in biomedical engineering from Politecnico di Milano, Milan Italy, in 2012, the M.S. degree in biomedical engineering, and the M.S.

and Ph.D. degrees in mechanical engineering, from the University of Florida in 2012, 2014, and 2015, respectively

He is currently a Postdoctoral Scholar at the Medical University of South Carolina. His research focuses on functional electrical stimulation, Lyapunov-based nonlinear control, and rehabilitation following stroke and spinal cord injury.

Dr. Downey is the recipient of the 2015 American Automatic Control Council (AACC) O. Hugo Schuck Best Paper Award.



Anup Parikh received the B.Sc. degree in both mechanical and aerospace engineering from the University of Florida, Gainesville, FL, USA. He is currently working towards the Ph.D. degree at the University of Florida under the advisement of Dr. Dixon.

As an undergraduate, he designed and fabricated a MEMS hot film shear stress sensor as an alternative to more expensive floating-element sensors. As a graduate researcher in the Nonlinear Controls and Robotics Group, his interests include vision-based estimation and control of UAV quadrotors and other

aerospace systems.



Warren E. Dixon received the Ph.D. degree from the Department of Electrical and Computer Engineering, Clemson University, Clemson, SC, USA, in 2000.

He was selected as an Eugene P. Wigner Fellow at Oak Ridge National Laboratory (ORNL). In 2004, he joined the Department of Mechanical and Aerospace Engineering, University of Florida, Gainesville, FL, USA. His main research interest has been the development and application of Lyapunov-based control techniques for uncertain nonlinear systems. He has published 3 books, an edited collection, 12 chapters,

and over 100 journal and 200 conference papers.

Dr. Dixon is the recipient of the 2009 and 2015 American Automatic Control Council (AACC) O. Hugo Schuck (Best Paper) Award, the 2013 Fred Ellersick Award for Best Overall MILCOM Paper, a 2012–2013 University of Florida College of Engineering Doctoral Dissertation Mentoring Award, the 2011 American Society of Mechanical Engineers (ASME) Dynamics Systems and Control Division Outstanding Young Investigator Award, the 2006 IEEE Robotics and Automation Society (RAS) Early Academic Career Award, an NSF CAREER Award (2006–2011), the 2004 Department of Energy Outstanding Mentor Award, and the 2001 ORNL Early Career Award for Engineering Achievement. He is an IEEE Control Systems Society (CSS) Distinguished Lecturer. He currently serves as a member of the U.S. Air Force Science Advisory Board and as the Director of Operations for the Executive Committee of the IEEE CSS Board of Governors.